Available online at www.sciencedirect.com
ScienceDirect
Trans. Nonferrous Met. Soc. China 31(2021) 3800−3813
Transactions of Nonferrous Metals Society of China
www.tnmsc.cn

Microstructure, tribological behavior and magnetic properties of Fe−Ni−TiO_2 composite coatings synthesized via pulse frequency variation

Ebrahim YOUSEFI[1,2], Shahriar SHARAFI[1], Ahmad IRANNEJAD[1]

1. Department of Materials Science and Engineering, Shahid Bahonar University of Kerman, 7618868366 Kerman, Iran;
2. Young Researchers Society, Shahid Bahonar University of Kerman, 7618868366 Kerman, Iran

Received 12 October 2020; accepted 23 July 2021

Abstract: The Fe−Ni−TiO_2 nanocomposite coatings were electrodeposited by pulse frequency variation. The results showed that the nanocomposite with a very dense coating surface and a nanocrystalline structure was produced at higher frequencies. By increasing the pulse frequency from 10 to 500 Hz, the iron and TiO_2 nanoparticles contents were increased in expense of nickel content. XRD patterns showed that by increasing the frequency to 500 Hz, an enhancement of BCC phase was observed and the grain size of deposits was reduced to 35 nm. The microhardness and the surface roughness were increased to 647 HV and 125 nm at 500 Hz due to the grain size reduction and higher incorporation of TiO_2 nanoparticles into the Fe−Ni matrix (5.13 wt.%). Moreover, the friction coefficient and wear rate values were decreased by increasing the pulse frequency; while the saturation magnetization and coercivity values of the composite deposits were increased.

Key words: Fe−Ni alloy coatings; electrodeposition; pulse frequency; tribomechanical properties; magnetic behaviors

1 Introduction

In recent decades, soft magnetic coatings have been widely applied in various electronic parts including magnetic heads, memory devices in computers, measurement transducers, sensors, electro valves, flux conductors and pole pieces in magnetic valves thanks to their excellent magnetic and suitable tribological properties [1−7]. However, in addition to excellent magnetic behavior, the soft magnetic coatings should have good mechanical properties for use in the mentioned applications [6−12]. Nevertheless, it has been observed that the Fe−Ni binary alloys cannot meet the required features in the electronic modern industry such as micro-electro-mechanical (MEMS) and nano-electro-mechanical systems (NEMS) due to low hardness and poor wear resistance [6−9].

Hence, to meet the ever-restricting industrial demands, the production of the deposits with good tribomechanical properties is of significance. In years old, the incorporation of inert ceramic particles during electrodeposition process and depositing of strengthened composites coatings with metal matrix are developed and caused to produce abrasion and corrosion-resistant advanced composite coatings [2,6−8]. In fact, it is observed that the co-deposition of neutral particle (such as carbides, oxides and nitrides) in the metal and alloy coatings leads to improving the growth process, physical and mechanical properties and also producing nanocrystalline deposits [2−3,8,13−15].

There are many various methods such as chemical and physical vapor deposition and thermal spraying that have already been introduced for the fabrication of alloy and composite coatings. Among these methods, the electrodeposition technique is a popular and known method for producing the alloy and composite coatings [2−4,11,16,17]. These

Corresponding author: Ebrahim YOUSEFI, Tel/Fax: +98-34-32114053, E-mail: e.yousefi@eng.uk.ac.ir
DOI: 10.1016/S1003-6326(21)65765-5

deposits are often deposited by direct current method, while pulsed current (PC) is utilized to a less extent. The coatings obtained by PC electrodeposition possess have better mechanical characteristics than those produced by direct current (DC) method. In fact, PC electrodeposition is an appropriate method to produce the coatings with low residual stress, high deposition rate, smooth surface, proper bonding between the matrix metal and ceramic particles, the advantages of high economic efficiency, and also with finer grains and more compact structures [2,3,14−18]. In the DC technique, the current density is the only variable parameter while in PC method, peak current density (J_p), on-time (t_{on}), off-time (t_{off}), duty cycle (d) and pulse frequency (f) are the independent variables that are able to control chemical composition and features of the deposited coatings [7−9,12,14]. The duty cycle corresponds to the percentage of total time of a cycle and is in the range of 1%−100%. Also, frequency is defined as the reciprocal of the cycle time [7,8,14,18].

Previous researches showed that by using the PC electrodeposition, the grain size is smaller than that of coatings produced by DC method and decreasing the grain size has the most significant effect on hardness and wear resistance [7−9,18]. Moreover, the strengthening mechanisms of polycrystalline metals and alloys are described as follows: (a) grain refinement strengthening (from Hall−Petch relationship); (b) dispersion strengthening (due to Orowan mechanism); (c) solid solution strengthening; (d) crystal orientation [3,18,19]. In the previous studies, the effects of composition and particle concentration of the plating bath and current density on the microstructure, mechanical and magnetic properties of the nanocomposite coatings on Fe−Ni matrix have been reported [6−8,15]. However, a few studies were done on the magnetic properties and tribological behaviors of Fe−Ni−TiO_2 nano-composite coatings.

In fact, different studies on the co-deposition of ceramic nanoparticles with iron−nickel matrix have been carried out due to the mechanical and tribological properties of these reinforcement particles (such as Al_2O_3 and SiC). But, there are not enough data on the structural and magnetic properties as well as the tribological behavior of Fe−Ni−TiO_2 composite coatings as a function of pulse frequency. As a result, this work has been carried out to study the nanocrystalline Fe−Ni−TiO_2 composite coatings produced by PC electro-deposition method from a sulfate bath. Also specifically, the effects of applied pulse frequency on the surface morphology, chemical composition, the amount of embedded nano-particles, phase structure, crystal size, magnetic properties, microhardness and tribological behaviors of these important engineering materials were investigated.

2 Experimental

2.1 Electrocodeposition

The Fe−Ni−TiO_2 nanocomposite coatings were obtained by PC electrodeposition from a sulfate bath. Copper samples and 430 stainless steel sheets were used as cathodes and the anodes, respectively. Moreover, the surface area of anode was chosen approximately three times greater than that of the cathode (dimensions of cathode and anode were 10 mm × 10 mm × 1 mm and 20 mm × 20 mm × 1 mm, respectively). Also, the surfaces of the substrates were mechanically polished with an abrasive paper from 800 to 3000 grade and then sequentially ultrasonically cleaned in acetone for 10 min. Then, they were cleaned with distilled water to remove contamination on the surface and immersed immediately in the plating bath to allow the co-deposition of the target nanocomposite coatings. The compositions of the sulfate plating bath and operating parameters are shown in Tables 1 and 2, respectively. Moreover, the electrolyte was prepared by dissolving reagents in distilled water.

Table 1 Chemical compositions of optimized sulfate plating bath for electrodeposition of Fe−Ni−TiO_2 coatings

Reagent	Concentration/($g \cdot L^{-1}$)
Ferrous chloride ($FeSO_4 \cdot 7H_2O$)	50
Nickel sulfate ($NiSO_4 \cdot 6H_2O$)	120
Nickel chloride ($NiCl_2 \cdot 6H_2O$)	25
Boric acid (H_3BO_3)	30
L-ascorbic acid ($C_6H_8O_6$)	3.5
Saccharin ($C_7H_5NO_3S$)	0.8
Sodium dodecyl sulfate ($C_{12}H_{25}SO_4Na$)	0.3
TiO_2 nanoparticles	35

Table 2 PC electrodeposition parameters for production of Fe−Ni−TiO_2 coatings

Electrodeposition parameter	Value
Pulse frequency/Hz	10, 50, 100, 250, 500
Current density/(mA·cm^{-2})	100
Duty cycle/%	50
Dimension of cathode/mm	10×10×1
Dimension of anode/mm	20×20×1
Temperature/°C	40±1
Stirring speed/(r·min^{-1})	300
pH	2.5−3

The pH value of the bath was maintained at 2.5−3 and controlled by using H_2SO_4 and NaOH solutions. The experiments were performed in a 100 mL plating cell containing 3.5 g of TiO_2 nanoparticles.

Direct current was supplied by a DC power supply unit (GP−4303D) and converted by a digital transformer to pulse current. The TiO_2 powder was purchased from US Nano Materials Research Company and the average particle size of the TiO_2 powder used in the experiments was about 30 nm. This commercial product consists of a mixture of the crystalline phases of anatase and rutile [8]. The nanoparticles were maintained as suspension in an electrolytic bath by continuous magnetic stirring at a rotating speed of 300 r/min for at least 12 h before co-deposition process. The suspension was subsequently agitated in an ultrasonic cleaner for 20 min just prior to the electroplating.

The nanocomposite coatings were fabricated using a pulse electrodeposition at a constant temperature of (40±1) °C and the solution was stirred during plating. Moreover, ascorbic acid was added as antioxidant to avoid anodic oxidation of Fe^{2+} to Fe^{3+}. Also, sodium dodecyl sulfate was used to disperse the particles in the electrolyte plating. The electric charge for plating each sample was kept constant at 50 C, which led to the same thickness in all coatings. Also, the corresponding deposition time was calculated from the Faraday's law. Thus, five composite coatings with fixed duty cycle (50%) and different frequencies (10, 50, 100, 250 and 500 Hz) were produced at a constant current density of 100 mA/cm^2. To avoid variations of the electrolyte composition, each bath was used only one time.

2.2 Characterization of deposits

The morphological characterization of the coatings was done using a Philips XL30 scanning electron microscope (SEM) and the element mass fraction of the samples was measured by energy dispersive X-ray (EDX) analyzer attached to the SEM. The final value of the mass fraction of each element in the composite coatings was reported as the average of three measurements performed at different locations of each specimen. Also, to investigate the nanoscale of coatings, the structural analysis of a specimen was conducted using TEM (Philips CM30). The structural analysis and grain size determination of the specimens were investigated by X-ray diffraction (XRD) technique using Cu K_α radiation (BRUKER/D8 ADVANCED diffractometer, 30 kV and 30 mA) and the results were interpreted by X-pert high score software. Also, the grain size (d) was calculated by using the Scherrer equation [8,13]:

$$d=0.9\lambda/(\beta\cos\theta) \quad (1)$$

where λ, β and θ are the wavelength of copper (λ=1.5406 Å), the full width at half-maximum (FWHM) of the peak and the diffraction angle, respectively. The scan was performed at 2θ values between 35° and 95° with a step size of about 0.03°. The hardness of the specimens was measured by a Vickers microhardness instrument at a constant applied load of 50 g for 15 s. The reported values were the average of 5 randomly located positions on the surface of each sample. The surface roughness of Fe−Ni−TiO_2 coatings has been measured by means of Stylus profilometer (Veeco Dektak 150). For this purpose, five measurements for each sample have been acquired and the mean value has been considered for the experience. The wear resistance of the coatings was determined using the wear testing instrument of pin-on-disk type and the applied vertical force was 3 N in dry conditions (production of Isfahan University of Technology Co., Iran). In this instrument, the sliding distance, movement radius and rotation speed were 300 m, 5 mm and 5 cm/s, respectively. Also, in this instrument, a pin of SAE 52100 hardened steel with a tip radius of 5 mm, a hardness of 800 HV, a height of 50 mm and a surface roughness of 0.01 mm was used. The wear rate values of the coatings were obtained from the difference in mass before and after wear testing by

carriage scales with 0.001 mg accurately. Also, the surface damage and worn surfaces caused by wear testing were subsequently analyzed by SEM images to get an idea about the wear mechanism. Magnetic properties of the deposits were measured by a vibrating sample magnetometer (VSM) (Lakeshor 7404, Co., USA). The dimensions of the samples used in the VSM measurements were 0.5 mm × 0.5 mm. Hysteresis loops were generated using a sweep time of 30 min at room temperature. Also, a parallel magnetic field of ±1.6 MA/m was applied on the surface of each sample.

3 Results and discussion

3.1 Morphological properties of deposits

The effect of pulse frequency on surface morphology of Fe−Ni−TiO_2 composite coatings is illustrated in Fig. 1. As shown in Fig. 1, the variation of the applied frequency has remarkable effect on the morphology of electroplated coatings. Also, the surfaces of the coatings are rough and very dense at higher pulse frequencies. The coatings have a mixture morphology including small nodular and cauliflower shaped ones [5,6,8,14,15]. The main reason for the formation of this morphology was attributed to the presence of Fe and Ni in the deposits. This issue has appeared in other works [5,6,8,14,15]. At higher pulse frequencies, the coatings were very rough with a large nodular and cauliflower shaped morphology. However, the dense structure and homogeneous morphology in all samples can be explained by the one step-using of PC electrodeposition processes and the presence of TiO_2 ceramic nanoparticles [6,8,12,15].

Moreover, the TEM micrograph of the electro-deposited sample at 500 Hz frequency is shown in Fig. 2. The edge of thin foil near the hole is the outer edge of the coating. It is reported that the bright region appears due to the local difference

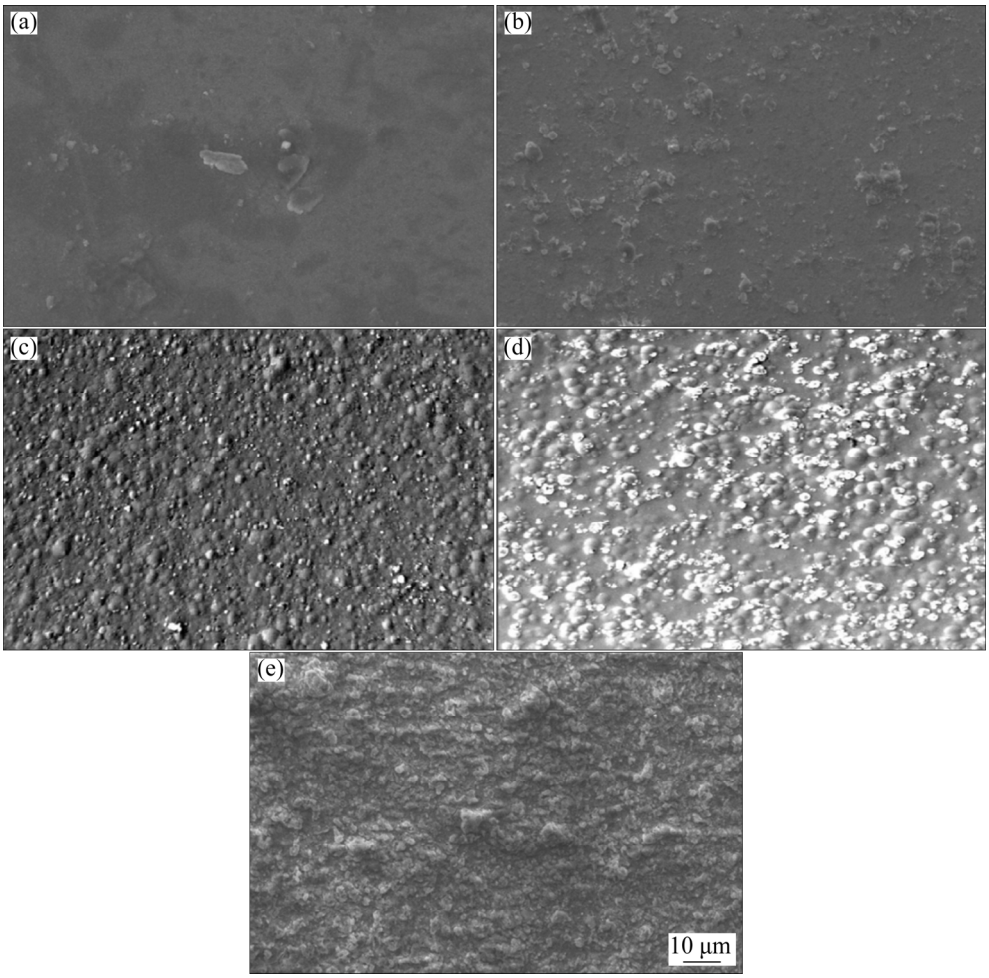

Fig. 1 SEM images of Fe−Ni−TiO_2 composite coatings obtained at different pulse frequencies: (a) 10 Hz; (b) 50 Hz; (c) 100 Hz; (d) 250 Hz; (e) 500 Hz

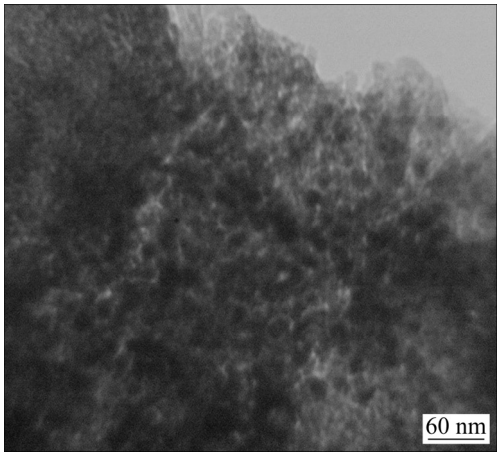

Fig. 2 TEM image of electrodeposited coating at 500 Hz

in the Fe content in the coating [1,4]. Also, it is observed that a nanocrystalline structure is produced and grains size is in the nanometer size. The crystallization process occurs either by the buildup of old crystals or with the nucleation and growth of new crystals. The competition between these two mechanisms with each other during the process and low surface diffusion rates, high contents of atoms and high overpotentials are the responsible parameters for the formation of new nuclei [8,13].

Different studies have shown that the variations in pulse frequency lead to change and refinement in grain size of the coatings. The times of charging and discharging cycles in the pulse on-time and off-time are very short at high frequencies. In fact, increasing the inclusion rate and decreasing the growth speed lead to the formation of dense and compact structures [7,18,20]. By formation of the nuclei on the surface, the grain growth is limited due to repeated interruption of the current density at high frequencies. Thus, so many nuclei are formed on the surface, which leads to grain size reduction and formation of fine-grained structures [7,11,18,20]. This behavior leads to decreasing the number of effective particles and increasing the roughness of the deposits. The nanoparticles have a higher tendency of agglomeration due to their high surface energy and activity than micro particles [3,8].

3.2 Chemical composition

The results of EDX in Fig. 3 exhibit that the applied frequency has a significant effect on the contents of Ni and Fe and the adsorption of TiO_2 nanoparticles. As shown in Fig. 3, with increasing the pulse frequency from 10 to 500 Hz, the contents of Fe and TiO_2 particles increase and the Ni content decreases. At the frequency of 500 Hz, the highest contents of Fe and TiO_2 are 72.5 and 5.2 wt.%, respectively. Also, the minimum content of Ni is 22.3 wt.%. This behavior is directly related to the increase in the concentration of iron ions near the cathode surface during the shorter silent pulse time [7,21]. This conclusion has the compatibility with new studies on the deposited coatings [6,7,21,22]. In the other researches, it was reported that the pulse frequency variation has not been effective on the chemical composition of Fe−Ni coatings [6,7,21].

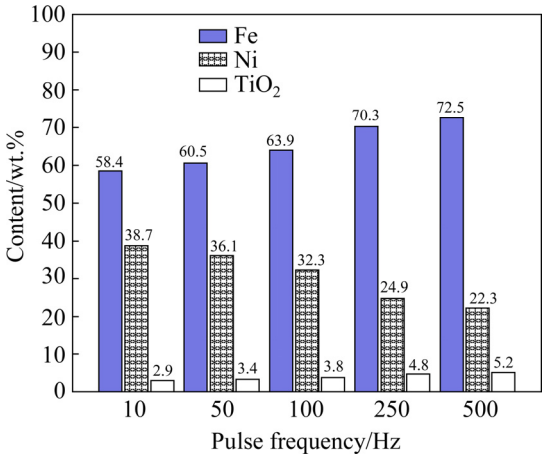

Fig. 3 Chemical compositions of Fe−Ni−TiO_2 composite coatings prepared at different pulse frequencies

In the new studies [6,7,21,22] it has been found that the change in pulse frequency has a direct effect on the mass fractions of Fe and Ni. SANATY-ZADEH et al [21] reported that increasing the frequency from 1000 to 16000 Hz leads to an increase in Fe content from 61 to 71 wt.%. This effect is explained by the increase in concentrations of Fe ions near the cathode surface during the pulse off-time.

On the other hand, applied pulse frequency plays an important role in the reinforcement of nanoparticles in the coatings. By increasing the pulse frequency at constant current density of 100 mA/cm^2 and duty cycle of 50%, the amount of nanoparticles embedded in the matrix increases. This behavior is due to the reduction of the off-time during the deposition process. By changing the applied pulse frequency from 10 to 500 Hz during electrodeposition process (at constant current

density of 100 mA/cm^2 and duty cycle of 50%), TiO_2 content embedded in the matrix significantly increases from 2.9 to 5.2 wt.%.

During prolonged off-time, the ceramic nanoparticles that have not yet adhered well to the cathode surface are excised and re-inserted into the electrolyte. Although the use of lower frequencies means longer cut-off time and this provides more opportunity for the ceramic nanoparticles to enter inside the dual layer, this behavior has been more likely to occur at very low frequencies between 1 and 0.1 Hz [7,18]. Another research has shown that during the off-time, the separation of poorly absorbed particles and the penetration of ceramic particles into the double-layer occur simultaneously. These two parameters compete with each other during the PC electrodeposition process, and each parameter prevails, determining the final effect. But, at higher off-time and pulse frequency, the deposition probability and the penetration of ceramic particles into the double-layer increase [7,20].

In general, the ceramic particles incorporation tends to increase with increasing of pulse frequency. This may be explained by the fact that the time duration of the imposed current in on-step is so long that the depletion of the electrolyte adjacent to the cathode surface occurs though the duty cycle is still at 50%. At lower frequencies, the higher reduction rate of metal ions in comparison with ions adsorbed on ceramic particles reduced the TiO_2 amount of the deposits. Moreover, at low frequencies due to the extensive off-time (t_{OFF}), loosely adsorbed nanoparticles could be removed by hydrodynamic forces. By increasing the applied pulse frequency, the off-time reduced and less loosely adsorbed TiO_2 nanoparticles could be detached [7,18,20]. Nevertheless, the highest amount of co-deposited nanoparticles in the coatings was 5.2 wt.%. By reduction of particle size, the co-deposition process of ceramic nanoparticles in the matrix is very difficult because, the ceramic nanoparticles are easily swept away from the cathode surface prior to the incorporation in metallic matrix of deposits. Thus, as seen in Fig. 3, the amount of TiO_2 nanoparticles embedded in the coatings was very low [3]. Moreover, EDX analysis results of Fe−Ni−TiO_2 coating prepared at a pulse frequency of 250 Hz are shown in Fig. 4, showing that there are Fe, Ni, Ti and O elements which have been formed Fe−Ni−TiO_2 composite coatings.

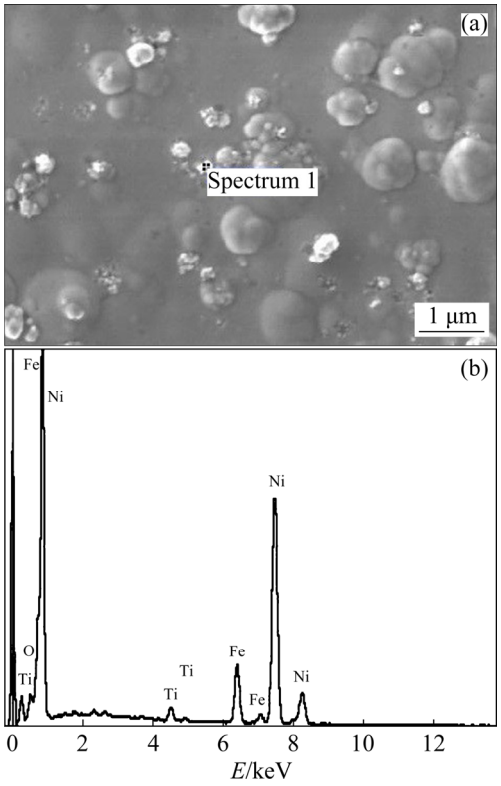

Fig. 4 SEM image (a) and EDX analysis results (b) of Fe−Ni−TiO_2 nanocomposite coatings at pulse frequency of 250 Hz

3.3 Structural characterization and XRD results

The XRD patterns of composite coatings prepared at different frequencies are illustrated in Fig. 5. As can be seen from this figure, the composite coatings exhibited two type lattices with different orientations which were influenced by the pulse frequency. In fact, a mixed phase structure of BCC and FCC crystals was observed for the deposited samples at pulse frequencies of 10, 50 and 100 Hz. However, by increasing the applied frequency, the phase structure of the coatings was changed. Accordingly, an enhancement in base-centered cubic phase fraction was observed due to an increase in Fe content of the coatings at frequencies of 250 and 500 Hz. This was well established that the structure of the deposited composites depends on the Fe amount [5,8,23]. This means that the applied frequency with change in chemical compositions of deposits has influenced the crystal structure of deposits and different solid solutions of Fe−Ni are formed. This behavior was confirmed in the previous studies [5,7,8,23]. It should be noticed that the peaks of TiO_2 with significant intensity were not detected in the XRD

patterns due to relatively high intensities of Fe and Ni diffraction peaks and very low content of the co-deposited TiO_2 nanoparticles in the Fe−Ni matrix.

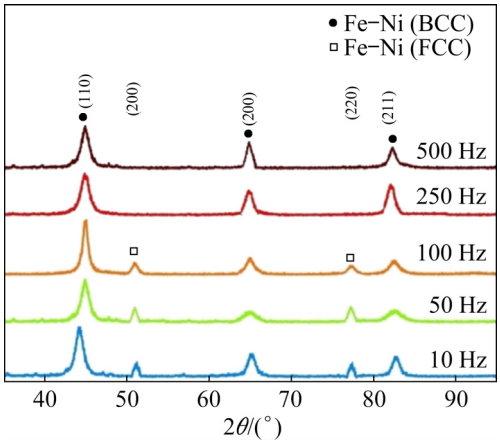

Fig. 5 Effect of pulse frequency on phase structure of Fe−Ni−TiO_2 composite coatings

Moreover, Scherrer method was used for the estimation of the crystallite size ((110) peak). The grain size values of Fe−Ni−TiO_2 composite coatings as a function of applied pulse frequency are shown in Fig. 6. The peak analyses of XRD patterns of composite coatings indicate a slight refinement of grain size with increasing pulse frequency. The slightness of this issue is due to the presence of TiO_2 particles which have already affected the grain size of the composite coatings [6,8,18]. In fact, the co-deposition of fine and small nanoparticles inside alloy matrix provides more nucleation sites by increasing the surface area of cathode. This effect prevents the grain growth and leads to the formation of deposits with smaller grain sizes [7,8,14,24,25]. Also, this refinement is due to the reduction of the on-time and enhancement of the nucleation rate at higher pulse frequencies.

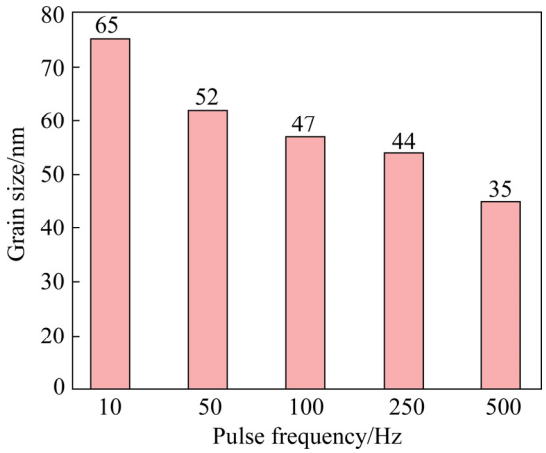

Fig. 6 Grain sizes of Fe−Ni−TiO_2 composite coatings at different pulse frequencies

It was observed that increasing the pulse frequency from 10 to 500 Hz led to the grain size reduction from 65 to 35 nm (at constant duty cycle and current density). The grain refinement due to the variation of applied pulse frequencies is the characteristic of the pulse electrodeposition technique [6,7,11]. In fact, with increasing the pulse frequency, the applied pulses are much shorter. This behavior can induce nanocrystalline structure and grain growth will be suppressed, and as a result, high frequency leads to the improvement of the mechanical properties [6,21].

3.4 Microhardness and surface roughness

Table 3 shows the variation of microhardness and surface roughness of Fe−Ni−TiO_2 coatings with applied pulse frequency. At higher frequencies, composite coatings exhibited higher hardness compared to those at lower frequencies (the highest microhardness was 647 HV at 500 Hz). It is reported that the increase in the Fe content leads to the enhancement of the mechanical properties [7,23]. Also, by increasing the content of Fe, a metallic phase with BCC structure is formed and this issue leads to a significant increase in microhardness [7,21]. This occurs for the coating prepared at 500 Hz as shown in Table 3. Moreover, this behavior is due to chemical composition variations and refinement mechanism of grain size of the deposits at higher applied frequencies.

Table 3 Variations of microhardness and surface roughness of Fe−Ni−TiO_2 coatings with pulse frequency

Sample No.	Pulse frequency/ Hz	Microhardness ($HV_{0.05}$)	Surface roughness/nm
1	10	543	48
2	50	568	71
3	100	589	92
4	250	612	103
5	500	647	125

In fact, structure refinement and grain size are affective parameters on improving the hardness of nanocrystal materials and coatings [7−9,20]. On the other hand, the longer off-time due to low applied

frequency (10 Hz) imposes on-time and off-time of 50 ms. The use of longer off-time provides the required time for the diffusion of iron and nickel ions into the crystal surface. This effect is good for crystals growth and produces a structure with rough grains [7,18,20]. While by increasing the frequency to 500 Hz, the off-time is very short due to the use of similar on-time and off-time (about 1 ms). Thus, the ceramic particles are diffused in the double-layer and this behavior leads to improving the properties of PC electrodeposits, and as a result, the hardness of the deposits increases at higher pulse frequencies [2,6−8,16,18].

Also, the higher microhardness at higher pulse frequencies is due to the co-deposition of TiO_2 hard particles and the strengthening mechanism of these inert nanoparticles. It is reported that embedded nanoparticles inside Fe−Ni matrix not only restrain the growth of the grains, but also decrease the plastic deformation by combined effects of the slight refinement of grain size and dispersive strengthening mechanisms [6−8,18,26,27]. Usually, the hardness of composite coatings is influenced by four important factors: (1) the chemical composition of metal matrix, (2) the amount of incorporated hard particles, (3) the refinement of the grains size, and (4) the phase structure [2,3,7,8,20].

The mean values of the surface roughness (R_a) of the studied deposits are represented in Table 3. The R_a values of the nanocomposite coatings are much higher in the coatings deposited at higher pulse frequencies. From Table 3, it is concluded that R_a values increase with high incorporation of TiO_2 reinforcing nanoparticles at higher applied frequencies. Thus, the surface roughness of the electrodeposited sample prepared at 500 Hz is noticeably enhanced as the highest content TiO_2 nanoparticles are incorporated into the coating (5.13 wt.%). This behavior between nanoparticles embedment and surface roughness is associated with reported results by other researchers [2,6,7,14]. On the other hand, the crystallite size is reduced with co-deposition of the reinforcing nanoparticles in Fe−Ni matrix (as seen in Fig. 6), and this issue is also a contributing parameter to R_a increment. It is confirmed that by increasing the numbers of nuclei and grains (crystallite size reduction) a significant increase in the surface roughness of deposits takes place [2,28]. Also, it is indicated that the surface roughness of Fe−Ni−TiO_2 composite coatings varies in the range from 48 to 125 nm.

3.5 Wear resistance and tribological behavior

3.5.1 Friction coefficient and wear rate of deposits

The effect of applied pulse frequency on the friction coefficient and the wear rate of Fe−Ni−TiO_2 composite coatings is presented in Fig. 7. It is observed that the samples prepared at higher pulse frequencies exhibit less friction coefficient and wear rate values and the sample prepared at 500 Hz has the best wear resistance (with the friction coefficient of about 0.59 and wear rate of about 0.55 μg/(N·m)). This behavior is due to higher amount of embedded TiO_2 nanoparticles and co-deposition of the coating with smaller grain sizes. In fact, by increasing the pulse frequency from 10 to 500 Hz, the content of TiO_2 nanoparticles in the matrix increases from 2.9 to 5.2 wt.%, while the grains size decreases from 65 to 35 nm. It is observed that the wear resistance of composite coatings is effectively influenced by the hardness, chemical composition and microstructure of metal matrix and the presence of nanoparticles inside deposits [3,7,11,16,29].

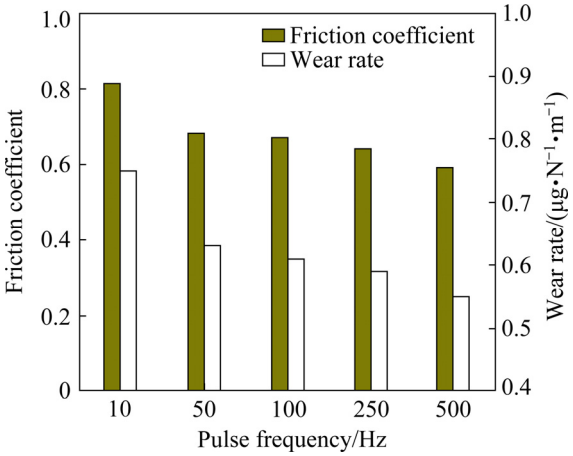

Fig. 7 Effect of pulse frequency on friction coefficient and wear rate of Fe−Ni−TiO_2 composite coatings

The amount of wear debris is more on the surface of Fe and Ni magnetic materials. However, wear debris plays the role of contact points between the surface of coating and abrasive pin, and as a result, the friction coefficient and wear rate values increased [8,30,31]. While the co-deposition of TiO_2 particles leads to the reduction of this direct contact during the wear process. On the other hand, these particles can play the role of a solid lubricant

between two abrasive surfaces, thus reducing the friction coefficient and wear rate [2,7,31,32]. Moreover, the movement of dislocations is encountered with difficulties owing to pile up of dislocations in nano-crystalline and fine-grained materials, which leads to the improvement of the tribological behavior [6−8,31,32]. Also, it has been reported that with the refinement and reduction of the grain size of the structure at high applied frequencies, the wear rate and friction coefficient of deposits decrease [2,3,7,33].

Furthermore, based on Archard's law, the wear volume during the wear process is directly proportional to the applied normal load, sliding distance for every cycle and the hardness of the coatings [7,9,34]. In fact, Archard's wear equation presented the relationship between the wear resistance and hardness of the materials that is shown in Eq. (2) [9,35,36]:

$$\Delta V=\frac{KLS}{H} \tag{2}$$

where ΔV is the wear volume, L is the normal load, S is the sliding distance for every cycle, H is the microhardness, and K is the coefficient of wear loss [9,35]. The effect of microhardness on the friction coefficient and mass loss values of the coatings is presented in Fig. 8. In this study, applied load (3 N) and sliding distance (300 m) were constant values for all examined specimens. Therefore, the relationship between ΔV and $1/H$ is linear. In fact, the microhardness of the deposits was believed to be the dominating parameter for the wear rate and coefficient of friction [9,35−37]. The

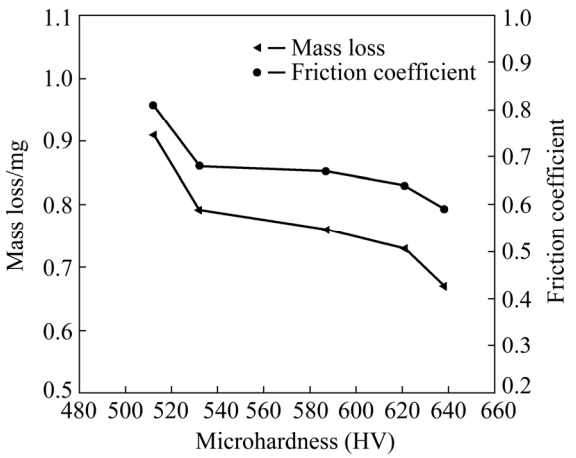

Fig. 8 Friction coefficient and mass loss values of coatings as function of microhardness

incorporation of TiO_2 nanoparticles in the matrix and the modification of grain growth lead to higher hardness of the composite coatings due to Orowan hardening mechanism [7,8,38,39]. According to the Archard's theory, the high hardness deposits are responsible and effective for reducing the friction coefficient, wear rate values and improving the tribological behavior of the specimens prepared at higher frequencies [7,8,35,36].

In general, the effect of applied pulse frequency on tribological behavior and mass loss values can be investigated from four standpoints.

(1) The coefficient of friction is decreased by increasing the amount of incorporated hard particles in the matrix. This behavior leads to reducing the wear rate due to decreasing the contact points between the surface of coating and abrasive pin and locking the surfaces.

(2) Increasing the amount of ceramic nanoparticles at high frequencies leads to difficulty in the movement of dislocations, and this increases the hardness and improves the anti-wear performance.

(3) One step-using of PC electrodeposition technique with high frequencies and the hard ceramic particles causes a fine grained and uniform microstructure. Thus, this behavior leads to the increase in the strength and hardness according to the Hall−Patch relationship.

(4) Increasing the pulse frequency leads to enhancing the compaction and surface density of the coatings, reducing the porosity, improving the co-deposition process of metal ions with ceramic nanoparticles and refining the grains size. As a result, this behavior causes a sharp reduction in the wear rate and improves the tribological behavior [6−9,38,39].

3.5.2 Wear mechanism

Figure 9 shows the scanning electron micrographs of worn surfaces for the specimens prepared at different pulse frequencies. From Fig. 9(a), it can be observed that the wear track width of this coating is far wide. Also, the adhesion effect is seen on the wear surfaces of the deposited sample at 10 Hz, which illustrates the dominance of adhesive wear mechanism. In other words, the deformed layers on the wear surfaces are related to the copper substrate due to low wear resistance and high penetration of abrasive pin in these coatings. Also, due to low wear resistance of this sample,

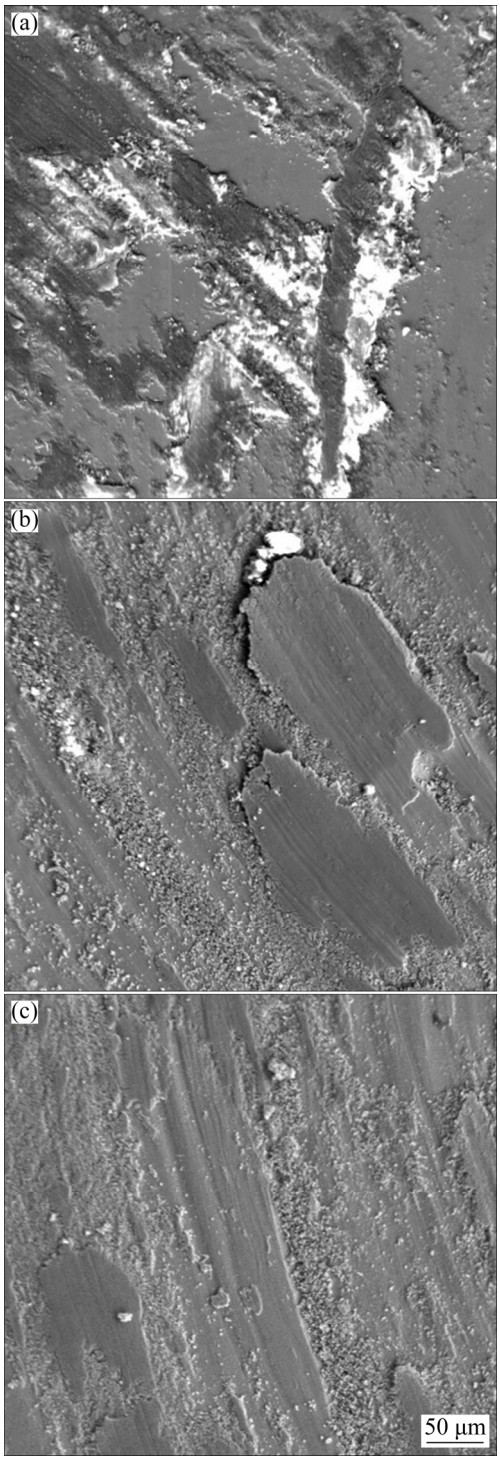

Fig. 9 SEM images of worn surfaces of coatings prepared at different pulse frequencies: (a) 10 Hz; (b) 100 Hz; (c) 500 Hz

wear particles and layers are separated from the surface and the wear debris in the similar zones to islands is seen on the worn surface. The presence of wear debris and adhesive wear mechanism can lead to higher friction coefficient and wear rate in this sample [8,40,41]. Moreover, it is observed that the the worn surface is not smooth due to adhesion or welding of Fe−Ni matrix with steel pin (Fig. 9(a)). Therefore, the worn surface initiates at 10 Hz with adhesive mechanism, plastic deformation and wear debris. This behavior is confirmed for Fe−Ni coatings in the previous studies [6,8,42].

But based on the SEM observations, the worn surfaces of deposited coatings with 100 and 500 Hz show that the continuous light scratches and grooves are created on the wear surfaces (Figs. 9(b) and (c)). The flattening and smearing on the wear scar are due to the plastic deformation [42,43]. It is severe abrasive effect in these samples and abrasive wear mechanism occurs. In fact, scratches are representative of abrasive wear mechanism. It is reported that during the ploughing process, the material is displaced on two sides of the abrasion groove without being removed [8,42,44]. Furthermore, the observed wear behavior can be explained by the higher hardness of these coatings [8,42]. As previously mentioned, the co-deposition of Fe, Ni and ceramic particles leads to the increase in the wear resistance and as a result, the wear debris and track width are decreased by an abrasive wear regime [6,8,14,24]. Comparing the worn surfaces of specimens prepared at different pulse frequencies clarifies this feature in Fig. 9. Also, it seems that the ploughed edges and deformed debris on the worn surfaces decrease, and also the penetration of pin in this sample is lower than that of the deposited sample prepared at 10 Hz. Moreover, it is evident that the specimens prepared at higher pulse frequencies exhibit better anti-wear performance, which can be attributed to the hard nature of reinforcements and the strengthening effect with incorporation of TiO_2 particles [8,24,32]. Therefore, these consequences demonstrate that the major wear mechanism is a mix of both adhesive and abrasive wear regimes for Fe−Ni−TiO_2 coatings.

3.6 Magnetic properties

It is well known that the magnetic behavior of the coatings depends on the chemical composition and grain size [5,8,13]. The magnetic properties of Fe−Ni−TiO_2 deposited coatings were measured at room temperature using VSM and the hysteresis curves of these samples are shown in Fig. 10. The magnetic measurements showed that the deposits exhibit soft magnetic properties because the hysteresis curves are narrow and the coercivity

values are smaller than 4800 A/m for all the specimens [8,13,45]. Also, the saturation magnetization (M_s) and coercivity (H_c) values of the coatings as a function of applied pulse frequencies are shown in Fig. 11. Higher M_s and H_c values of the specimens prepared at higher frequencies may be explained by variations of composition and grains size of the deposits. As seen in Fig. 11, the M_s values increase with increasing the applied frequency. This is related to the decrease of Ni content and increase of Fe content in the deposits [5,7−9,46]. Also, it is reported that the saturation magnetization is inversely proportional to TiO_2 content which is a non-magnetic compound (with paramagnetic behavior) [8]. But, the effect of higher Ni content overcomes this effect at higher frequencies.

Furthermore, the grain size is one of the effective parameters on the coercive field [5,8,9,13]. The H_c value is found to increase constantly with

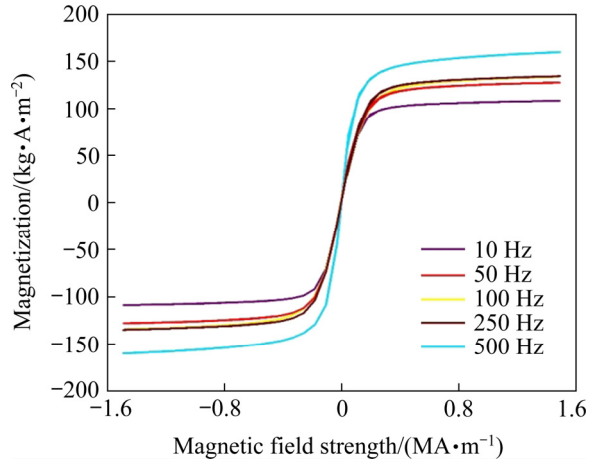

Fig. 10 Hysteresis curves of coatings at different pulse frequencies

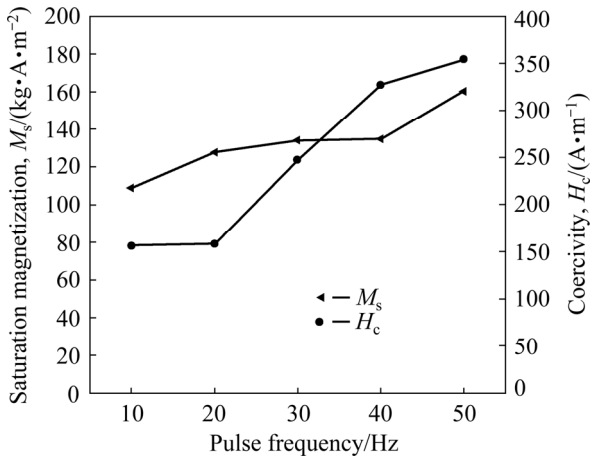

Fig. 11 Saturation magnetization and coercivity of coatings at different pulse frequencies

applied frequency as shown in Fig. 11. This result is due to the grain size reduction at high frequencies and also, this behavior is in agreement with the Herzer theory. In the similar researches it is shown that a decrease in grain size leads to higher H_c values at grain sizes above magnetic exchange length [8,9,13,45]. In fact, the random anisotropy model (RAM) was presented to investigate the dependence of H_c on the average grain size (D) and magnetic exchange length (L_{ex}) [8,47]. The L_{ex} is calculated according to Eq. (3):

$$L_{ex}=\sqrt{\frac{A}{K_1}} \tag{3}$$

where A and K_1 are the exchange stiffness and the magneto-crystalline anisotropy constants, respectively [8,13,48].

Based on the random anisotropy model, the H_c varies according to Eq. (4):

$$H_c=\frac{P_c D^6 {K_1}^4}{\mu_0 M_s A^3} \tag{4}$$

where P_c is a constant of the order of unity, and μ_0 is the permeability of free space [8,13,48,49].

It is reported that when $D>L_{ex}$, the H_c has an inverse relationship with the grain size and generally, a smaller grain size leads to an increase in the coercivity [13,47−49]. The ferromagnetic exchange length is decreased by Fe content reduction and the L_{ex} is between 14 and 28 nm for Fe−Ni permalloy deposits [8,47,49]. In this study, the grain size of the samples is larger than the magnetic exchange length. Thus, the increase of coercivity values is due to the grain size reduction according to the random anisotropy model.

Unlike M_s, the coercivity H_c is an extrinsic property and depends on many factors including the grain size, phase structure and chemical composition [5,7−9,13]. As seen from XRD patterns in Fig. 5, the phase transformation from mixed BCC and FCC phase structures to single BCC phase occurs with an increase in the applied frequencies. It is reported that the material with single BCC phase shows higher coercivity values compared to that with FCC structure [5,13,45]; while, the formation of mixed phase leads to the decrease in coercivity (at 10, 50 and 100 Hz). Moreover, increasing the co-deposition rate of TiO_2 nanoparticles in the Fe−Ni matrix leads to increasing the coercivity values due to grain size

reduction of the coatings [8]. Generally, it is observed that the grain size and coercivity values show inverse dependence with each other.

4 Conclusions

(1) The surface of the coatings is compact and very dense at high pulse frequencies. TEM images demonstrate that a nanocrystalline micro- structure is obtained due to the co-deposition of TiO_2 nanoparticles, repeated interruption of the current density and restriction of grain growth at high frequencies.

(2) Increasing the frequency from 10 to 500 Hz leads to the increase of the amount of Fe and TiO_2 particles by increasing concentrations of Fe ions near the cathode surface during pulse off-time and reduction of the off-time in the deposition process. Also increasing the pulse frequency to 250 and 500 Hz leads to increasing the Fe−Ni (BCC) solid solution peak intensities at the expense of those belonging to Fe−Ni (a mixed phase structure of BCC and FCC crystals) ones. Moreover, higher pulse frequency has a positive effect on grain refinement due to the reduction of the on-time and the enhancement of the nucleation rate.

(3) The composite coatings show higher hardness at higher applied frequencies. This is due to the decrease in the off-time, higher incorporation of TiO_2, the formation of a BCC phase structure and the refinement of the grain size of the deposits.

(4) The crystallite size reduction and inclusion of rough TiO_2 nanoparticles inside the matrix are contributing factors for the increment of the surface roughness at higher pulse frequencies. Moreover, the surface roughness of Fe−Ni−TiO_2 deposits varies in the range of 48−125 nm.

(5) The sample prepared at 500 Hz provides the most appropriate tribomechanical properties with the friction coefficient of about 0.59 and the wear rate of 0.55 μg/(N·m). The main wear mechanism observed is a mix of both adhesive and abrasive wear regimes mainly noticed at higher applied frequencies.

(6) The coercivity has an almost inverse dependence with grain size of the coatings. Also, the saturation magnetization and coercivity values increase due to increasing the Fe content, the formation of a BCC phase structure, the high co-deposition rate of the nanoparticles and the grain size reduction at high pulse frequencies.

References

[1] CHEN Z H, YANG X, FU Y. Influence of sodium propargyl sulfonate on electrodeposition of Fe−Co alloy [J]. Journal of Alloys and Compounds, 2020, 826: 154167.

[2] RASOOLI A, SAFAVI M S, BABAEI F, ANSARIAN A. Electrodeposited Ni−Fe−Cr_2O_3 nanocomposite coatings: A survey of influences of Cr_2O_3 nanoparticles loadings in the electrolyte [J]. Journal of Alloys and Compounds, 2020, 822: 153725.

[3] CHAUDHARI A K, SINGH V B. A review of fundamental aspects, characterization and applications of electrodeposited nanocrystalline iron group metals, Ni−Fe alloy and oxide ceramics reinforced nanocomposite coatings [J]. Journal of Alloys and Compounds, 2018, 751: 194−214.

[4] GAO L Y, WAN P, LIU Z Q. Gradient growth of FCC and BCC phase within Fe_xNi_{1-x} ($50<x<75$) films during direct-current wafer electroplating [J]. Journal of Magnetism and Magnetic Materials, 2020, 498: 166131.

[5] PAVITHRA G P, HEGDE C H. Magnetic property and corrosion resistance of electrodeposited nanocrystalline iron–nickel alloys [J]. Applied Surface Science, 2012, 258: 6884−6890.

[6] TORABINEJAD V, ROUHAGHDAM A S, ALIOFK-HAZRAEI M, ALLAHYARZADEH M H. Electrodeposition of Ni−Fe and Ni−Fe-(nano Al_2O_3) multilayer coatings [J]. Journal of Alloys and Compounds, 2016, 657: 526−536.

[7] TORABINEJAD V, ALIOFKHAZRAEI M, ASSAREH S, ALLAHYARZADEH M H, ROUHAGHDAM A S. Electrodeposition of Ni−Fe alloys, composites, and nano coatings—A review [J]. Journal of Alloys and Compounds, 2017, 691: 841−859.

[8] YOUSEFI E, SHARAFI S H, IRANNEJAD A. The structural, magnetic, and tribological properties of nanocrystalline Fe−Ni permalloy and Fe−Ni−TiO_2 composite coatings produced by pulse electro co-deposition [J]. Journal of Alloys and Compounds, 2018, 753: 308−319.

[9] YOUSEFI E, SHARAFI S H, IRANNEJAD A. Electrodeposition and characterization of nanocrystalline Fe−Ni−Cr alloy coatings synthesized via pulse current method [J]. Transactions of Nonferrous Metals Society of China, 2019, 29: 2591−2603.

[10] GUL H, KILIC F, UYSAL M, ASLAN S, ALP A, AKBULUT H. Effect of particle concentration on the structure and tribological properties of submicron particle SiC reinforced Ni metal matrix composite (MMC) coatings produced by electrodeposition [J]. Applied Surface Science, 2012, 258: 4260−4267.

[11] SIAHPOOSH H, ABBASI A, ALIOFKHAZRAEI M, KHAJAVI B, MAJIDI H. Effect of pulse frequency on tribological behaviour of functionally graded Ni/Al_2O_3 nanocomposite coatings [J]. Procedia Materials Science, 2015, 11: 498−502.

[12] ADELKHANI H, ARSHADI M R. Properties of Fe−Ni−Cr alloy coatings by using direct and pulse current

electrodeposition [J]. Journal of Alloys and Compounds, 2009, 476: 234−237.

[13] GHAFERI Z, SHARAFI SH, BAHROLOLOOM M H. Effect of current density and bath composition on crystalline structure and magnetic properties of electrodeposited FeCoW alloy [J]. Applied Surface Science, 2015, 355: 766−773.

[14] PARIDA G, CHAIRA D, CHOPKAR M K, BASU A. Synthesis and characterization of Ni−TiO_2 composite coatings by electro-co-deposition [J]. Surface and Coating Technology, 2011, 205: 4871−4879.

[15] ATAEE-ESFAHANI H, VAEZI M R, NIKZAD L, YAZDANI B, SADRNEZHAAD S K H. Influence of SiC nanoparticles and saccharin on the structure and properties of electrodeposited Ni−Fe/SiC nanocomposite coatings [J]. Journal of Alloys and Compounds, 2009, 484: 540−544.

[16] LANZUTTI A, LEKKA M, LEITENBURG C D, FEDRIZZI L. Effect of pulse current on wear behavior of Ni matrix micro- and nano-SiC composite coatings at room and elevated temperature [J]. Tribology International, 2019, 132: 50−61.

[17] ALLAHYARZADEH M H, ALIOFKHAZRAEI M, ROUHAGHDAM A S, ALIMADADI H, VAHID T. Mechanical properties and load bearing capability of nanocrystalline nickel−tungsten multilayered coatings [J]. Surface and Coating Technology, 2020, 386: 125472.

[18] LAJEVARDI S, ASHAHRABI T. Effects of pulse electrodeposition parameters on the properties of Ni−TiO_2 nanocomposite coatings [J]. Applied Surface Science, 2010, 256: 6775−6781.

[19] AAL A. Hard and corrosion resistant nanocomposite coating for Al alloy [J]. Materials Science and Engineering A, 2008, 474: 181−187.

[20] YANG Y, CHENG F. Fabrication of Ni−CO−SiC composite coatings by pulse electrodeposition—Effects of duty cycle and pulse frequency [J]. Surface and Coating Technology, 2013, 216: 282−288.

[21] SANATY-ZADEH A, RAEISSI K, SAIDI A. Properties of nanocrystalline iron−nickel alloys fabricated by galvano-static electrodeposition [J]. Journal of Alloys and Compounds, 2009, 485: 402−407.

[22] CHUNG C K, CHANG W T. Effect of pulse frequency and current density on anomalous composition and nanomechanical property of electrodeposited Ni−Co films [J]. Thin Solid Films, 2009, 517: 4800−4804.

[23] EBRAHIMI F, LI H. Structure and properties of electrodeposited nanocrystalline FCC Ni−Fe alloy [J]. Reviews on Advanced Materials Science, 2003, 5: 134−138.

[24] CHEN L, WANG L P, ZENG Z X, ZHANG J Y. Effect of surfactant on the electrodeposition and wear resistance of Ni−Al_2O_3 composite coatings [J]. Materials Science and Engineering A, 2006, 434: 319−325.

[25] THIEMIG D, LANGE R, BUND A. Influence of pulse plating parameters on the electrocodeposition of matrix metal nanocomposites [J]. Electrochimica Acta, 2007, 52: 7362−7371.

[26] BAHROLOLOOM M E, YOUSEFI-SANI R. The influence of pulse plating parameters on the hardness and wear resistance of nickel–alumina composite coatings [J]. Surface and Coating Technology, 2005, 192: 154−163.

[27] KATAMIPOUR A, FARZAM M, DANAEE I. Effects of sonication on anticorrosive and mechanical properties of electrodeposited Ni−Zn−TiO_2 nanocomposite coatings [J]. Surface and Coating Technology, 2014, 254: 358−363.

[28] TRIPATHI M, SINGH V B, SINGH H K. Structure and properties of electrodeposited functional Ni−Fe/TiN nanocomposite coatings [J]. Surface and Coating Technology, 2015, 278: 146−156.

[29] HOU K H, CHEN Y C. Preparation and wear resistance of pulse electrodeposited Ni−W/Al_2O_3 composite coatings [J]. Applied Surface Science, 2011, 257: 6340−6346.

[30] HUANG Z J, XIONG D S. MoS_2 coated with Al_2O_3 for Ni−MoS_2/Al_2O_3 composite coatings by pulse electro-deposition [J]. Surface and Coating Technology, 2008, 202: 3208−3214.

[31] MAHDAVI S, ALLAHKARAM S R. Composition, characteristics and tribological behavior of Cr, Co−Cr and Co−Cr/TiO_2 nano-composite coatings electrodeposited from trivalent chromium based baths [J]. Journal of Alloys and Compounds, 2015, 635: 150−157.

[32] BAGHERY P, FARZAM M, MOUSAVI A B, HOSSEINI M. Ni−TiO_2 nanocomposite coating with high resistance to corrosion and wear [J]. Surface and Coating Technology, 2010, 204: 3804−3810.

[33] SEO M H, KIM D J, KIM J S. The effects of pH and temperature on Ni−Fe−P alloy electrodeposition from a sulfamate bath and the material properties of the deposits [J]. Thin Solid Films, 2005, 489: 122−129.

[34] CHAUDHARI A, SINGH V. Structure and properties of electro-co-deposited Ni−Fe/ZrO_2 nanocomposites from ethylene glycol bath [J]. International Journal of Electrochemical Science, 2014, 9: 7021−7037.

[35] ZHOU Y B, ZHAO G G, ZHANG H J. Fabrication and wear properties of co-deposited Ni−Cr nanocomposite coatings [J]. Transactions of Nonferrous Metals Society of China, 2010, 20: 104−109.

[36] SHEIBANI-AGHDAM A, ALLAHKARAM S R, MAHDAVI S. Corrosion and tribological behavior of Ni−Cr alloy coatings electrodeposited on low carbon steel in Cr(III)−Ni(II) bath [J]. Surface and Coating Technology, 2015, 281: 144−149.

[37] PRIYAN S H, AZAD A, ARAFFATH Y. Influence of HVOF parameters on the wear resistance of Cr_3C_2−NiCr coating [J]. Journal of Materials Science and Surface Engineering, 2016, 4: 355−359.

[38] KARATALA M, UYSAL M, GUL H, ALP A, AKBULUT H. Effect of surfactant concentration in the electrolyte on the tribological properties of nickel−tungsten carbide composite coatings produced by pulse electro co-deposition [J]. Applied Surface Science, 2015, 345: 328−336.

[39] XU S H, QIU J W, ZHANG H B, CAO H Z, ZHENG G Q, LIU Y. Friction behavior of Ti−30Fe composites strengthened by TiC particles [J]. Transactions of Nonferrous Metals Society of China, 2021, 31: 988−998.

[40] HADIPOUR A, MONIRVAGHEFI S M. Comparison of H−Cr single layer and Ni−P/H−Cr duplex coating [J]. Surface Engineering, 2015, 31: 666−672.

[41] MADADI F, SHAMANIAN M, ASHRAFIZADEH F. Effect of pulse current on microstructure and wear resistance of

stellite 6/tungsten carbide claddings produced by tungsten inert gas process [J]. Surface and Coating Technology, 2011, 205: 4320−4328.

[42] TORABINEJAD V, ALIOFKHAZRAEI M, ROUHAGHDAM A S, ALLAHYARZADEH M H. Tribological properties of Ni−Fe−Co multilayer coatings fabricated by pulse electrodeposition. [J]. Tribology International, 2017, 106: 34−40.

[43] WANG Y, LIE Z, WANG T, HUI X D, CHEN W, FENG C. Effect of sliding velocity on the transition of wear mechanism in $(Zr,Cu)_{95}Al_5$ bulk metallic glass [J]. Tribology International, 2016, 101: 141−151.

[44] ALLAHYARZADEH M H, ALIOFKHAZRAEI M, ROUHAGHDAM A S, TORABINEJAD V. Electro-deposition of Ni−W−Al_2O_3 nanocomposite coating with functionally graded microstructure [J]. Journal of Alloys and Compounds, 2016, 666: 217−226.

[45] SAKITA A, PASSAMANI E C, KUMAR H, CORNEJO R C, FUGIVARA C S, NOCE R D, BENEDETTI A V. Influence of current density on crystalline structure and magnetic properties of electrodeposited Co-rich CoNiW alloys [J]. Materials Chemistry and Physics, 2013, 141: 576−581.

[46] KOO B, YOO B. Electrodeposition of low-stress NiFe thin films from a highly acidic electrolyte [J]. Surface and Coating Technology, 2010, 205: 740−744.

[47] JING P P, LIU M T, PU Y P, CUI Y F, WANG Z, WANG J B, LIU Q F. Dependence of phase configurations, microstructures and magnetic properties of iron–nickel (Fe−Ni) alloy nanoribbons on deoxidization temperature in hydrogen [J]. Scientific Reports, 2016, 6: 1010−1038.

[48] BAHRAMI A H, SHARAFI S H, AHMADIAN-BAGHBADERANI H. The effect of Si addition on the microstructure and magnetic properties of permalloy prepared by mechanical alloying method [J]. Advanced Powder Technology, 2013, 24: 235−241.

[49] WEN C H, CHEN Z, HUANG B, RONG Y. Nanocrystallization and magnetic properties of Fe−30wt.% Ni alloy by surface mechanical attrition treatment [J]. Metallurgical and Materials Transactions A, 2006, 37: 1413−1421.

脉冲频率变化制备 Fe−Ni−TiO_2 复合涂层的显微组织、摩擦学行为和磁性能

Ebrahim YOUSEFI[1,2], Shahriar SHARAFI[1], Ahmad IRANNEJAD[1]

1. Department of Materials Science and Engineering, Shahid Bahonar University of Kerman, 7618868366 Kerman, Iran;
2. Young Researchers Society, Shahid Bahonar University of Kerman, 7618868366 Kerman, Iran

摘　要：利用脉冲频率变化电沉积 Fe−Ni−TiO_2 纳米复合涂层。结果表明，在较高的频率下可以制备出表面致密、具有纳米晶结构的涂层。当脉冲频率从 10 Hz 增加到 500 Hz，涂层中 Fe 和 TiO_2 纳米颗粒含量增加，Ni 含量降低。XRD 结果显示，当频率增加到 500 Hz，BCC 相的峰强度增加，沉积物的晶粒尺寸减小至 35 nm。而且，由于晶粒尺寸减小和 Fe−Ni 基体中 TiO_2 纳米颗粒的掺入率较高(5.13 wt.%)，显微硬度和表面粗糙度分别达到 647 HV 和 125 nm。另外，脉冲频率增大，复合涂层的摩擦因数和磨损率减小，饱和磁化强度和矫顽力均增加。

关键词：Fe−Ni 合金涂层；电沉积；脉冲频率；摩擦学性能；磁性能

(Edited by Wei-ping CHEN)